Integrin signaling modes controlling cell migration and metastasis

Truong, H.H.

Chapter 7

Integrin control of ZEB/miR-200 balance regulates tumor cell migration strategy and metastasis

Truong HH, Ghotra VPS, Nirmala E, Le Dévédec SE, van der Helm D, Lalai R, He S, Ewa Snaar-Jagalska BE, Amiet A, Marcinkiewicz C, Vreugdenhil E, Meerman JHN, van de Water and Danen EHJ. *Submitted for publication*

Integrin control of ZEB/miR-200 balance regulates tumor cell migration strategy and metastasis

Hoa Truong[1], Veerander PS Ghotra[1], Ella Nirmala[1], Sylvia E Le Dévédec[1], Danny van der Helm[1], Reshma Lalai[1], Shuning He[2], B. Ewa Snaar-Jagalska[2], Alex Amiet[3], Cezary Marcinkiewicz[4], Erno Vreugdenhil[5], John HN Meerman[1], Bob van de Water[1], and Erik HJ Danen[1*]

[1]Division of Toxicology and [5]Division of Medical Pharmacology, Leiden Amsterdam Center for Drug Research, and [2]Department of Molecular Cell Biology, Institute of Biology, Leiden University, Leiden NL; [3]Thermofischer Scientific, Lafayette CO; [4]Department of Biology, Temple University, Philadelphia PA

[*]Corresponding author: Division of Toxicology, LACDR, Leiden University, Leiden NL. e.danen@lacdr.leidenuniv.nl

Cellular interactions with the extracellular matrix (ECM) are mediated by transmembrane receptors of the integrin family, which coordinate signal transduction cascades impinging on cell survival, proliferation, and migration[1]. Interactions through β1 integrins support initiation and growth of breast and skin cancers and β1 antibodies sensitize breast tumors in mice to radiotherapy[2-4]. Here, we show that peptide blocking or gene silencing of β1 integrins can also cause a switch from cohesive multicellular strand invasion to individual cell migration in 3D matrices and in a zebrafish xenograft model where β1 integrin depletion promotes breast cancer cell spreading. In an orthotopic mouse transplantation model, tumor growth of β1 integrin-depleted breast cancer cells is reduced, but intravasation and lung metastasis of cells from these small tumors is strongly enhanced. Depletion of β1 integrins alters the balance between miR-200 microRNAs (miRNAs) and ZEB transcriptional repressors resulting in a transcriptional downregulation of E-cadherin, which is essential for the induction of individual cell migration and enhanced metastasis. These findings demonstrate that disturbed integrin-mediated interactions with the ECM in cancer cells can attenuate tumor growth but also alter cell migration strategies leading to increased metastasis through a miRNA-transcription factor network that controls cell-cell adhesion.

A panel of breast epithelial cell lines was microinjected into collagen gels where they formed tumor cell spheroids within the first day and cell migration was analyzed over the next 4 days. MTLn3 and MDA-MB-231 carcinoma cells, which lack E-cadherin-mediated cell-cell contacts in 2D culture, migrated into the collagen as single cells; a process here referred to as "*individual cell migration*" (not shown). MCF10a immortalized epithelial cells and 4T1 carcinoma cells, both forming E-cadherin-mediated intracellular junctions in 2D, invaded the collagen gel as multicellular strands; here referred to as "*cohesive invasion*" (Fig 1A, S1; Mov S1). We asked how integrin-mediated ECM attachment regulates cohesive invasion of cells with a relatively stable epithelial phenotype (MCF10A) and transformed cells displaying a mix of epithelial and mesenchymal characteristics (4T1). Silencing β1 integrins in MCF10a blocked invasive capacity whereas 4T1shβ1 spheroids lost the ability to invade as cohesive strands but instead

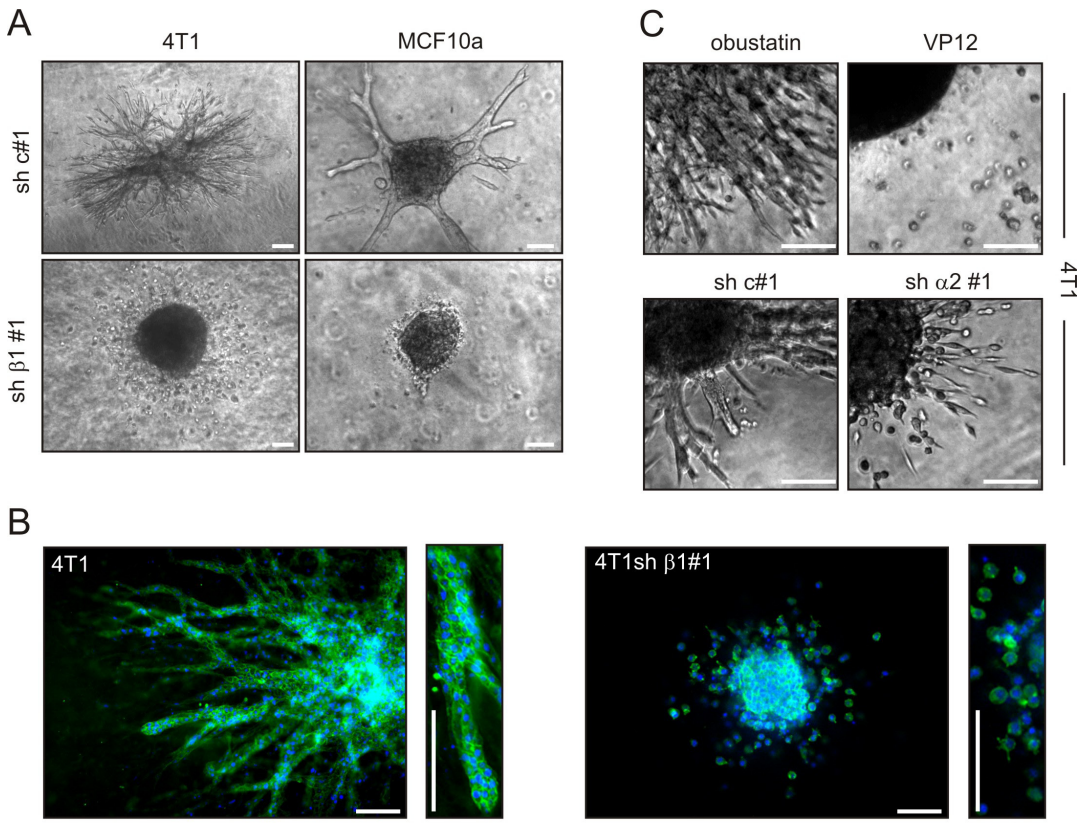

Figure 1. Integrin control of 3D migration patterns. A, spheroids of 4T1 and MCF10a cells expressing indicated shRNAs 4 days post-injection in collagen gels. **B,** E-cadherin staining of 4T1 and 4T1shβ1 spheroids 4 days post-injection in collagen gels. **C**, spheroids of 4T1 cells in the presence of indicated peptides (top) or expressing indicated shRNAs (bottom) 4 days post-injection in collagen gels. Scale bars, 50 μm.

tumor cells was strongly increased for 4T1shβ1 tumors as compared to control tumors (Fig 2C). We further analyzed the in vivo migratory capacity using a xenograft model where tumor cells were injected in the yolk sac of zebrafish embryos and spreading throughout the embryo was quantified. Again, silencing β1 integrins led to an increased ability to migrate away from the primary tumor cell mass and travel to distant sites in the body (Fig 2D-F). When cells were injected into the developing blood system of these embryo's they rapidly became trapped in the vasculature and, in agreement with the migration patterns observed in 3D collagen matrices, wild type 4T1 cells showed cohesive outgrowth in those regions whereas 4T1shβ1 cells spread in a non-cohesive fashion (Fig S5).

We compared gene expression profiles in β1 knockdown and control 4T1 cells. Using a false discovery rate (FDR) <0.001 and 1.5-fold difference as a cut-of, 1230 differentially expressed genes were shared between both shβ1 lines (Table S1). In this set, Ingenuity Pathway Analysis predicted "*cellular movement*" as the process most significantly affected by β1 integrin silencing and also predicted *"cell-to-cell signaling"*. Both processes contained the *Cdh1* gene that was significantly downregulated in both shβ1 lines but not in the sh-control line, which was confirmed by qPCR (Fig 3A, S6). Indeed, silencing β1 integrins in 4T1 caused a

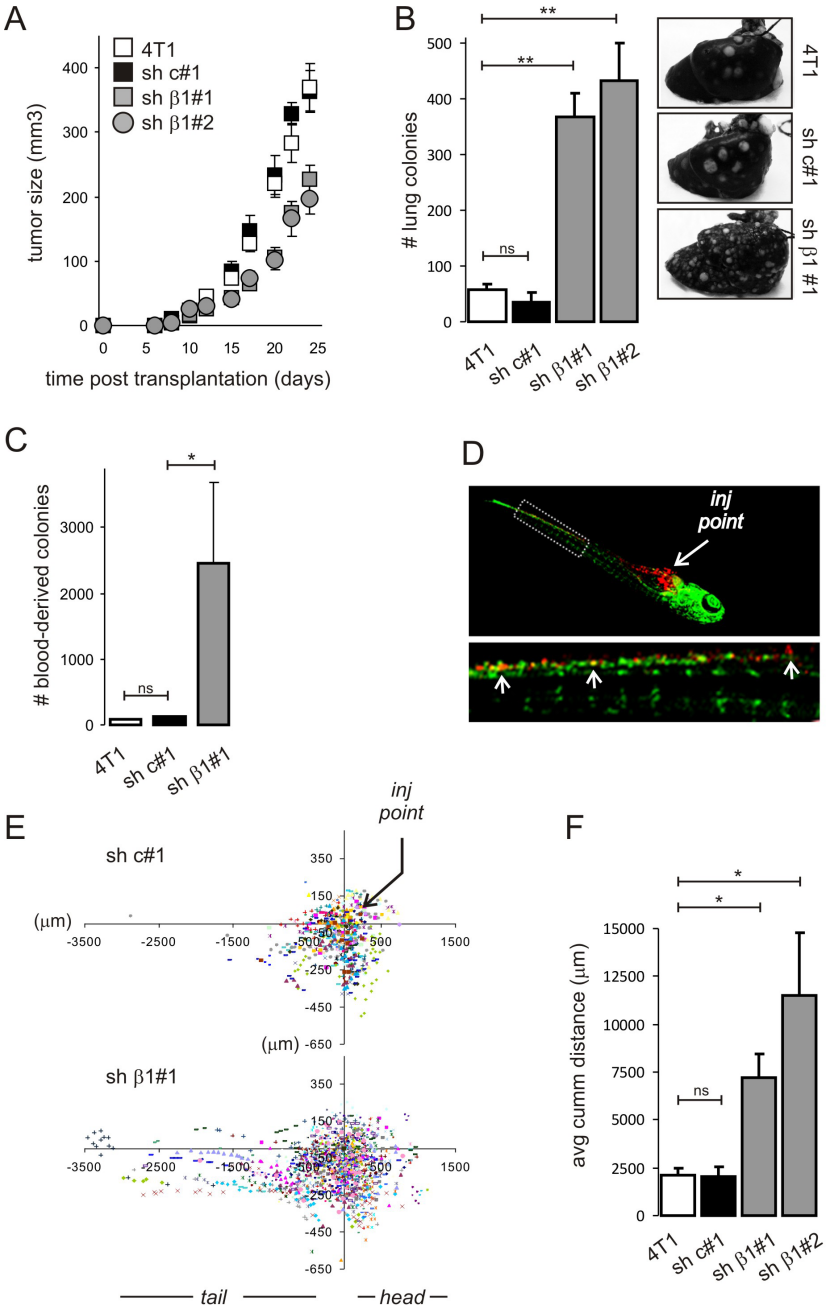

Figure 2. Integrin control of in vivo migration. A-C, primary tumor growth (**A**), spontaneous metastasis (**B**), and circulating tumor cells (**C**) following orthotopic transplantation of 4T1 cells expressing indicated shRNA constructs in mammary fat pad (>25 mice per condition from 3 independent experiments). **D**, CM-DiI labeled 4T1shβ1 cells injected in zebrafish yolk sac (top) and spread towards tail region 5 days post-injection (bottom). **E**, graphic representation of tumor cell spreading in ~40 zebrafish embryos per condition taken from 2 independent experiments (each pattern/color depicts tumor cells in a single embryo) in which labeled 4T1 cells expressing indicated shRNAs were injected in yolk sac. **F**, average of cumulative migration distances of tumor cells per embryo, calculated from E. *p<0.05; **p<0.001.

~75% reduction in E-cadherin surface expression and a similar trend was observed upon α2 silencing (Fig 3B). β1 silencing also diminished total E-cadherin protein levels and E-cadherin was reduced in primary tumors derived from 4T1shβ1 cells as compared to control tumors (Fig 3C,D). Notably, in agreement with their inability to switch to an individual cell migration mode (Fig 1A), silencing β1 integrins in MCF10a did not affect E-cadherin surface expression (Fig 3B).

There is evidence that integrin-mediated ECM adhesion can modulate cell-cell adhesion and both positive and negative regulation has been reported but crosstalk at the level of E-cadherin expression has not been demonstrated[9-11]. A very recent report showed that low levels of α2β1 integrin in human breast cancer are associated with poor survival[12]. This association was confirmed in the same "NKI 295" set but not in a larger, pooled breast cancer cohort from The Netherlands Cancer Institute, Amsterdam, NL[13] or in an independent breast cancer cohort from Erasmus University Rotterdam, NL[14] (not shown). Global expression of α2 or β1 was not associated with E-cadherin expression and associations detected in sub-groups were not corroborated in each cohort (not shown). This indicates that reduced expression of β1 integrins is not a general phenomenon in breast cancer, which may not be surprising given their dual role in growth and migration. Cell-ECM interactions can also be locally altered in tumors by changes in integrin activity or surface levels, or by altered proteolytic ECM degradation. Our findings indicate that such events can lead to transient E-cadherin downregulation in tumor cells already on the edge of EMT, allowing a subset of tumor cells to escape from the primary tumor mass and metastasize to distant organs.

We tested if the reduction in E-cadherin expression levels was critically involved in the pro-metastatic switch in cell migration strategy upon β1 integrin silencing. In support of this, ectopic expression of E-cadherin in 4T1shβ1 at similar surface levels as found in control 4T1 cells, restored cohesive invasion (Fig 3E, S7). It also blocked lung metastasis of 4T1shβ1 tumors (Fig 3F) whereas E-cadherin expression did not affect tumor growth, which was slow in β1 integrin-depleted tumors irrespective of the absence or presence of E-cadherin, further demonstrating that integrins control tumor growth and metastasis through separate pathways (Fig 3G).

Having established that the ability of β1 integrins to control E-cadherin levels can critically affect metastatic behavior, we investigated the mechanism by which β1 integrins control E-cadherin expression. Luciferase reporter assays showed that β1 integrin silencing led to a ~80% transcriptional downregulation of the *Cdh1* gene (Fig 4A). This prompted us to investigate regulation of a group of E-cadherin transcriptional repressors, including members of the Snail, bHLH, and ZFH families that are implicated in EMT[15]. Analysis of the micro-array data showed that of these repressors, only Zeb2 (also known as Sip1) was significantly and specifically upregulated in both 4T1shβ1 lines and qPCR confirmed the induction of Zeb2, but not Zeb1, upon β1 integrin silencing (Fig 4B, S6). ZEBs act as transcriptional repressors of miRNAs of the miR-200 family, which are expressed from two clusters on two distinct chromosomes. Vice versa, miR-200 family members post-transcriptionally repress Zeb1 and Zeb2 by targeting their 3' UTRs. This ZEB/miR-200 feedforward loop has been implicated in EMT, and alterations in the balance between ZEB and miR-200 may underlie progression of a number of different types of cancer, including breast carcinomas[16-18]. miRNA profiling indicated a strong downregulation of all five members of the miR-200 family in β1 integrin-

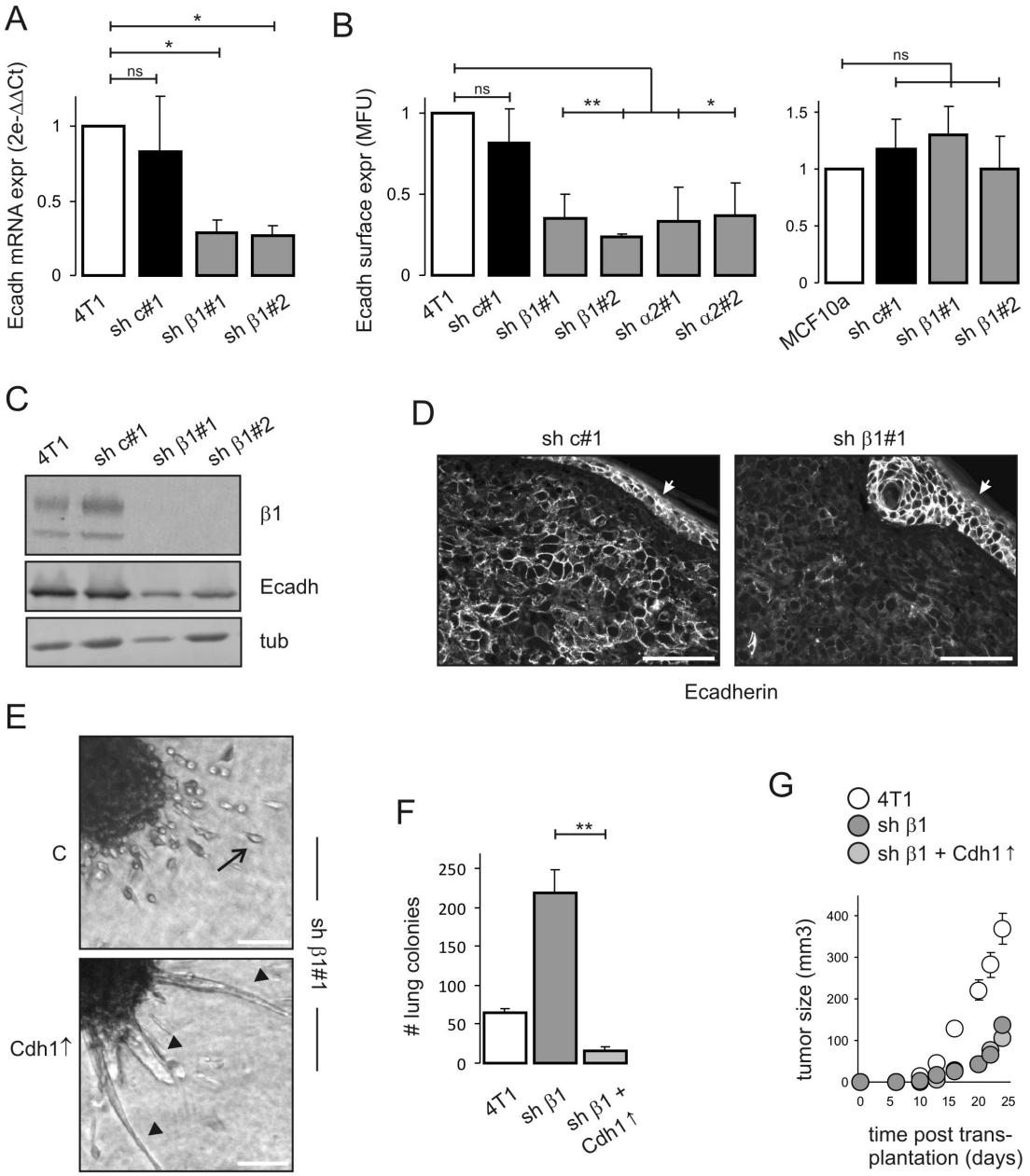

Figure 3. Suppression of E-cadherin is critical for integrin regulation of invasion and metastasis. A-C, E-cadherin mRNA (q-PCR) (**A**), surface expression (FACS) (**B**), and total protein (**C**) levels in 4T1 or MCF10a cells expressing indicated shRNAs. **D**, E-cadherin staining in 4T1 and 4T1shβ1 orthotopic breast tumors (arrow indicates skin, which serves as positive control in both). **E**, spheroids of 4T1shβ1 cells without (top) or with E-cadherin cDNA (bottom) 4 days post-injection in collagen gels (arrow indicates individual cell migration; arrow heads point to cohesive invasion strands). **F-G**, Lung metastasis (**F**) and primary tumor growth (**G**) of orthotopically transplanted 4T1 cells expressing indicated shRNAs and cDNAs (>20 mice per condition from 2 independent experiments). Scale bars, 50 μm. *p<0.05; **p<0.001.

depleted, but not control shRNA cells (Fig 4C).

We investigated the significance of miR-200 suppression for the observed β1 integrin-mediated control of the mode of invasion. Synthetic or lentiviral expression of any individual miR-200 family member restored cell-cell adhesion in 2D cultures of 4T1shβ1 cells and induced a reversal to cohesive 3D migration (Fig 4D, S8, S9, and data not shown). On the other hand, none of the miRNA hairpin inhibitors targeting miR-200 family members was able to interfere with cell-cell adhesion in wild type 4T1 cells (not shown). Together, these data point to overlapping functions of the miR-200 family members in this system and demonstrate that downregulation of all five members is required for the observed inhibition of cohesion upon depletion of β1 integrins. We noted that expression of each miR-200 expression construct was invariably lost within 5 days after GFP sorting, suggesting that the expression of mature miR-200 species caused a growth disadvantage (not shown). Finally, restored cell-cell adhesion upon expression of miR-200 family members in 4T1shβ1 cells was accompanied by a downregulation of Zeb2, concomitant with an upregulation of E-cadherin (Fig 4E), further pointing to a central role for Zeb2/miR-200 in β1 integrin-mediated control of E-cadherin based cohesion.

Altogether, our findings establish a novel connection between integrin-mediated cell-ECM interactions and E-cadherin-mediated adherens junctions. Interfering with β1 integrin-mediated ECM adhesion attenuates tumor growth but it can also disturb the ZEB/miR-200 balance leading to E-cadherin downregulation. This triggers a switch from cohesive to individual cell migration, which we find to act pro-metastatic in an orthotopic breast cancer model. The findings raise concerns with respect to the use of integrins as drug targets to sensitize tumors to radio- or chemotherapy. They also point to a new cross talk mechanism between cell-ECM and cell-cell adhesions that may regulate transient loss of cohesion in subpopulations of cancer cells within tumors where EMT has not been documented. While E-cadherin is almost invariably lost in invasive lobular breast carcinomas its expression is retained in many other types including the common ductal invasive carcinomas[19,20]. In those cases, a transient downregulation of E-cadherin through disturbed tumor cell-ECM interactions in a minor population of invading cells may drive metastasis while going unnoticed.

METHODS SUMMARY

4T1 mouse breast cancer cells and MCF10a human mammary epithelial cells were transduced using lentiviral shRNA or cDNA vectors and selected for integrin or E-cadherin surface expression by bulk FACS sorting. Synthetic miRNA Mimics and Hairpin Inhibitors were transfected at 50 nM, cells were replated next day, and used for FACS, qPCR, or collagen invasion 48 hours later. Cells expressing lentiviral miRNA shMIMICS were selected by bulk FACS sorting for GFP. E-cadherin firefly luciferase reporter[21] was transfected with CMV-renilla luciferase reporter and cells were analyzed using dual luciferase assay kit 3 days later. For 3D invasion, cell suspensions were microinjected into collagen gels followed by DIC imaging or immunostaining for F-actin or E-cadherin. Disintegrins and C-lectin type proteins, including Obustatin (α1β1), VLO4 (α5β1; αvβ3), VLO5 (α4β1; α9β1) and VP12 (α2β1), were used at 4.6 μM[5]. For orthotopic tumor growth, cells were injected into the fat pad of recipient mice

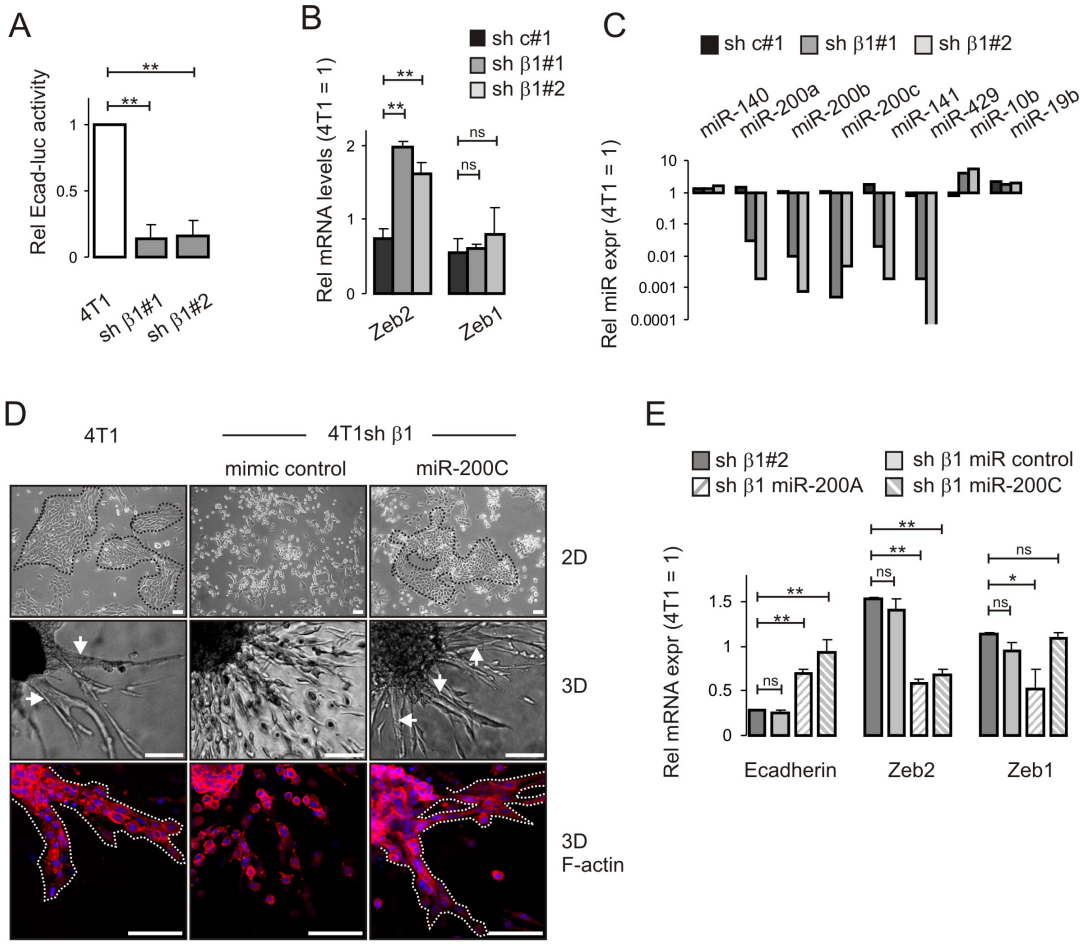

Figure 4. Integrin regulation of miR-200/ZEB balance controls E-cadherin expression and cohesive migration. A-B, E-cadherin promoter activity (luc assay) (**A**) and Zeb1 and Zeb2 mRNA levels (qPCR) (**B**) in 4T1 cells expressing indicated shRNAs. **C**, Relative levels of miRNAs in 4T1 expressing indicated shRNAs (qPCR array). **D**, 4T1 cohesion suppressed by shβ1 and restored by synthetic miR-200C Mimic in 2D culture (top) and in 3D collagen gels (middle and bottom) (arrows point to cohesive invasion strands). **E**, E-cadherin, Zeb2, and Zeb1 mRNA levels in 4T1shβ1 cells expressing indicated synthetic miRNA Mimics. Scale bars, 50 μm. *p<0.05; **p<0.001.

and tumor size was monitored. Affter 3-4 weeks, animals were anesthetized, primary tumor and lungs were excised for immunostaining and spontaneous metastasis counting, and in some cases blood was drawn for circulating tumor cells. For zebrafish xenotransplantation experiments, labeled tumor cells were injected into the yolk sac or developing vascular system of Fli-GFP transgenic zebrafish embryos. Embryos were maintained at 34°C for 6 days, and cumulative distance of spread tumor cells was calculated from confocal images. Real-time qPCR data were expressed using 2^(-ΔΔCt) method. Taqman microRNA qPCR assay kit was used for miRNA profiling. Affimetrix MG430 PM Array plates were used for micro-arrays. Differentially expressed genes were identified using random-variance t-test after quality

control and median normalization. Western blot and FACS were done as described[22]. Data are presented as mean ± SEM of at least 3 independent biological replicates unless otherwise stated. Student's t test (two-tailed) was used to compare groups.

REFERENCES

1. Hynes RO. (2002). Integrins: bidirectional, allosteric signaling machines. *Cell* 110, 673-687.
2. Reuter JA, Ortiz-Urda S, Kretz M, Garcia J, Scholl FA, Pasmooij AM, et al. (2009) Modeling inducible human tissue neoplasia identifies an extracellular matrix interaction network involved in cancer progression. *Cancer Cell* 15:477-88.
3. White DE, Kurpios NA, Zuo D, Hassell JA, Blaess S, Mueller U, et al. (2004) Targeted disruption of beta1-integrin in a transgenic mouse model of human breast cancer reveals an essential role in mammary tumor induction. *Cancer Cell* 6:159-70.
4. Park CC, Zhang H, Pallavicini M, Gray JW, Baehner F, Park CJ, et al. (2006) Beta1 integrin inhibitory antibody induces apoptosis of breast cancer cells, inhibits growth, and distinguishes malignant from normal phenotype in three dimensional cultures and in vivo. *Cancer Res* 66:1526-35.
5. Staniszewska I, Walsh EM, Rothman VL, Gaathon A, Tuszynski GP, Calvete JJ, Lazarovici P, Marcinkiewicz C. (2009) Effect of VP12 and viperistatin on inhibition of collagen receptors-dependent melanoma metastasis. *Cancer Biol Ther* 8:1-10.
6. Sahai,E. and Marshall,C.J. (2003). Differing modes of tumour cell invasion have distinct requirements for Rho/ROCK signalling and extracellular proteolysis. *Nat. Cell Biol.* 5, 711-719.
7. Friedl P, Wolf K. Plasticity of cell migration: a multiscale tuning model. (2010). *J Cell Biol* 188:11-19.
8. Shibue T, Weinberg RA. (2009) Integrin beta1-focal adhesion kinase signaling directs the proliferation of metastatic cancer cells disseminated in the lungs. *Proc Natl Acad Sci USA* 106:10290-10295.
9. Monier-Gavelle F, Duband JL. (1997) Cross talk between adhesion molecules: control of N-cadherin activity by intracellular signals elicited by beta1 and beta3 integrins in migrating neural crest cells. *J Cell Biol* 137:1663-81.
10. Weaver VM, Petersen OW, Wang F, Larabell CA, Briand P, Damsky C, et al. Reversion of the malignant phenotype of human breast cells in three-dimensional culture and in vivo by integrin blocking antibodies. J Cell Biol 1997; 137:231-45.
11. de Rooij J, Kerstens A, Danuser G, Schwartz MA, Waterman-Storer CM. (2005) Integrin-dependent actomyosin contraction regulates epithelial cell scattering. *J Cell Biol* 171:153-64.
12. Ramirez NE, Zhang Z, Madamanchi A, Boyd KL, O'Rear LD, Nashabi A, Li Z, Dupont WD, Zijlstra A, Zutter MM J. (2010) The alpha2beta1 integrin is a metastasis suppressor in mouse models and human cancer. *J Clin Invest.* 42328.
13. Reyal F, van Vliet MH, Armstrong NJ, Horlings HM, de Visser KE, Kok M, Teschendorff AE, Mook S, van 't Veer L, Caldas C, Salmon RJ, van de Vijver MJ, Wessels LF. (2008) A comprehensive analysis of prognostic signatures reveals the high predictive capacity of

the proliferation, immune response and RNA splicing modules in breast cancer. *Breast Cancer Res.* 10 R93.
14. Wang Y, Klijn JG, Zhang Y, Sieuwerts AM, Look MP, Yang F, Talantov D, Timmermans M, Meijer-van Gelder ME, Yu J, Jatkoe T, Berns EM, Atkins D, Foekens JA. (2005) Gene-expression profiles to predict distant metastasis of lymph-node-negative primary breast cancer. *Lancet* 365: 671–679.
15. Thiery JP. (2002) Epithelial-mesenchymal transitions in tumour progression. *Nat Rev Cancer* 2:442-54.
16. Bracken CP, Gregory PA, Kolesnikoff N, Bert AG, Wang J, Shannon MF, Goodall GJ. (2008) A double-negative feedback loop between ZEB1-SIP1 and the microRNA-200 family regulates epithelial-mesenchymal transition. *Cancer Res* 68:7846-54.
17. Gregory PA, Bert AG, Paterson EL, Barry SC, Tsykin A, Farshid G, Vadas MA, Khew-Goodall Y, Goodall GJ. (2008) The miR-200 family and miR-205 regulate epithelial to mesenchymal transition by targeting ZEB1 and SIP1. *Nat Cell Biol* 10:593-601.
18. Calin GA and Croce CM. (2006) MicroRNA signatures in human cancers. *Nat Rev Cancer* 6:857-66.
19. Moll R, Mitze M, Frixen UH, Birchmeier W. (1993) Differential loss of E-cadherin expression in infiltrating ductal and lobular breast carcinomas. *Am J Pathol* 143:1731-1742.
20. Berx G, Cleton-Jansen AM, Nollet F, de Leeuw WJ, van de Vijver M, Cornelisse C, et al. (1995) E-cadherin is a tumour/invasion suppressor gene mutated in human lobular breast cancers. *Embo J* 14:6107-6115.
21. Comijn J, Berx G, Vermassen P, Verschueren K, van Grunsven L, Bruyneel E, Mareel M, Huylebroeck D, van Roy F. (2001) The two-handed E box binding zinc finger protein SIP1 downregulates E-cadherin and induces invasion. *Mol Cell* 7:1267-1278.
22. Danen,E.H., Sonneveld,P., Brakebusch,C., Fassler,R., and Sonnenberg,A. (2002). The fibronectin-binding integrins alpha5beta1 and alphavbeta3 differentially modulate RhoA-GTP loading, organization of cell matrix adhesions, and fibronectin fibrillogenesis. *J. Cell Biol.* 159, 1071-1086.

ACKNOWLEDGEMENTS

We thank Dr. Patrick Derksen (UMC, Utrecht NL) for sharing the E-cadherin expression vector, Dr. Geert Berx (VIB, Gent BE) for providing the E-cadherin luciferase reporter, Drs Sander Canisius and Lodewijk Wessels (NKI, Amsterdam NL) and Marcel Smid and John Martens (Erasmus MC, Rotterdam NL) for bioinformatics analysis of breast cancer patient cohorts, Dr. Gabby Krens for introduction to the microinjection protocol, Dr. Marjo de Graauw for critical reading of the manuscript, and Ms Wies van Roosmalen for assistance with mouse experiments. HT was supported by the Dutch Cancer Society (UL-2010-4670). VPSG and SH were supported by EU FP7 (HEALTH-F2-2008-201439).

AUTHOR CONTRIBUTIONS

HT, VPSG, EN, and DvdH performed and analyzed in vitro experiments. HT, SELD, and RL performed and analyzed mouse experiments. VPSG and SH performed and analyzed zebrafish experiments. CM isolated disintegrins. EV and JHNM assisted in miRNA profiling and microarray data analysis. AA generated synthetic and lentiviral miRNA reagents. BvdW and BES were involved in discussions and writing of the manuscript. HT and EHJD planned experiments, discussed results, and wrote the manuscript. All authors critically read the manuscript. The authors declare no competing financial interests.

SUPPLEMENTARY TABLE, FIGURE, AND MOVIE LEGENDS

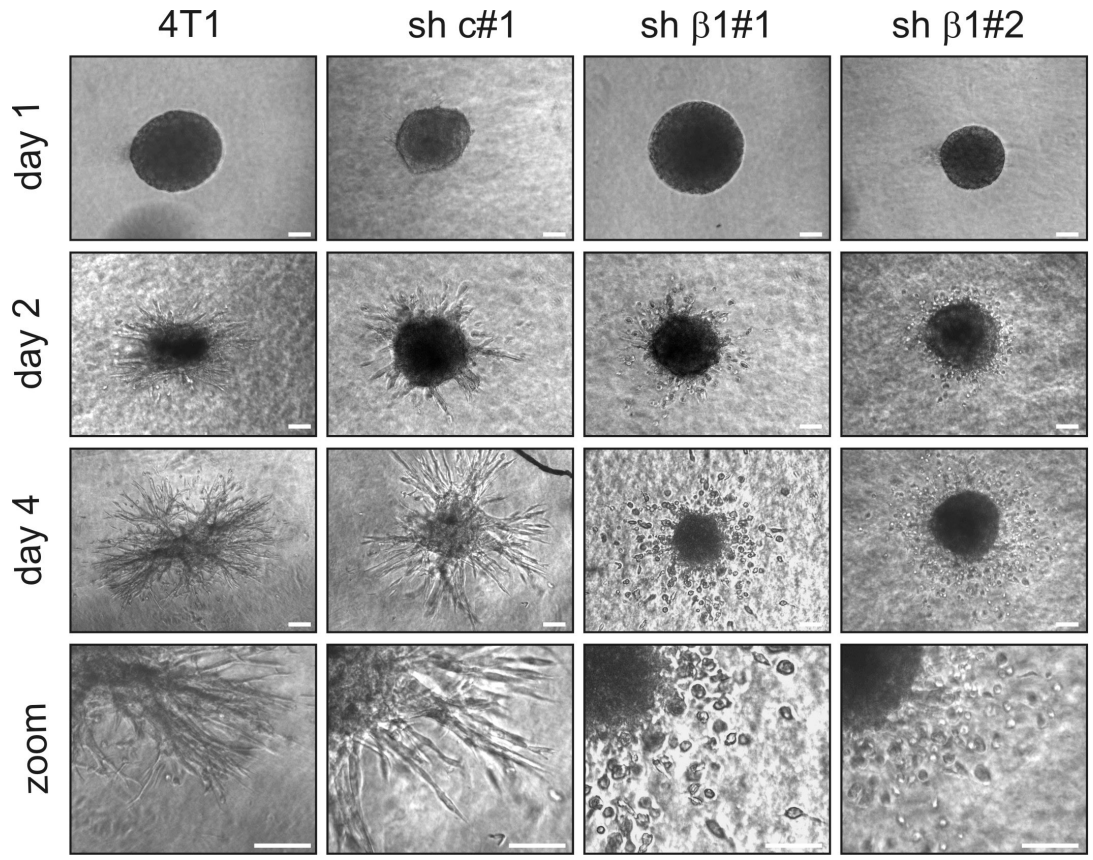

Figure S1. Spheroids of 4T1 cells expressing indicated shRNAs at indicated timepoints post-injection in collagen gels. Scale bars, 50 μm.

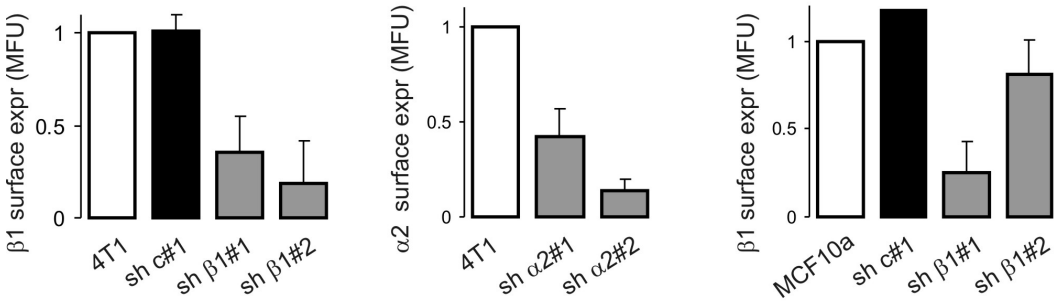

Figure S2. FACS analysis of β1 or α2 integrin surface expression in 4T1 or MCF10a cells expressing indicated shRNAs.

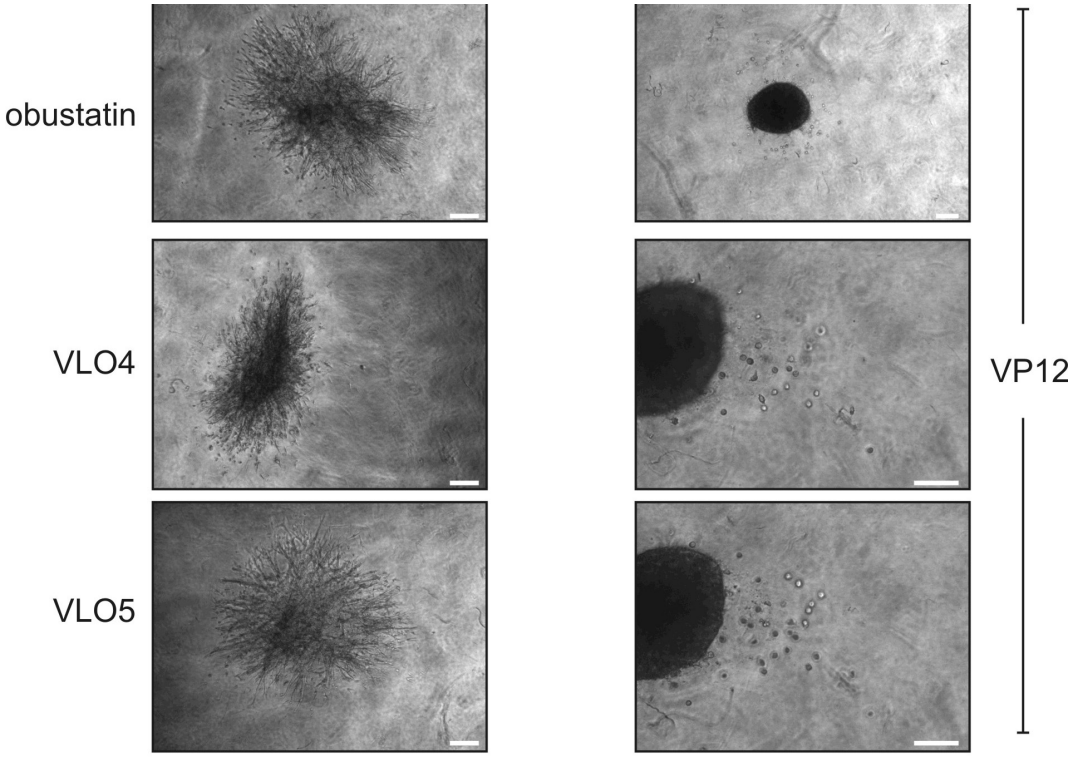

Figure S3. Spheroids of 4T1 cells in the presence of indicated peptides 4 days post-injection in collagen gels. Scale bars, 50 μm.

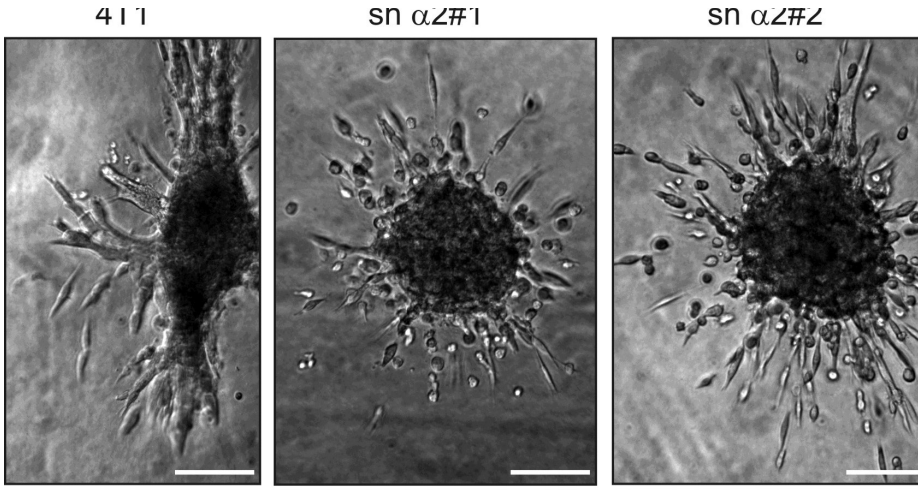

Figure S4. Spheroids of 4T1 cells expressing indicated shRNAs 4 days post-injection in collagen gels. Scale bars, 50 μm.

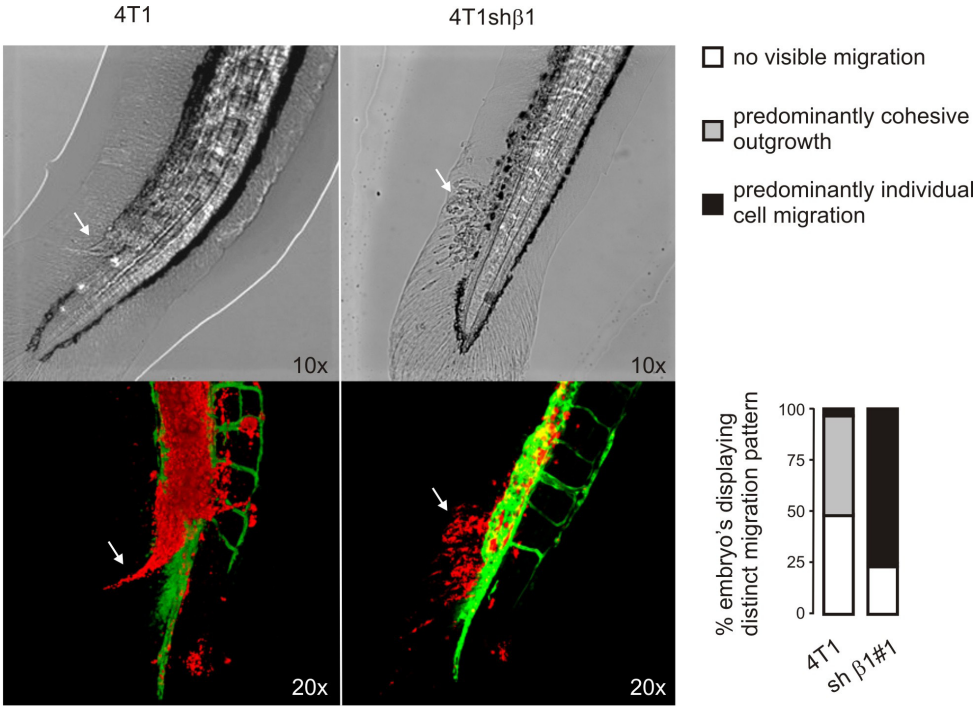

Figure S5. Cohesive outgrowth of wild type 4T1 cells (left image) versus non-cohesive spreading of 4T1shβ1 cells (right image) 3 days post-injection into the developing blood system of zebrafish embryos. DIC (top) and confocal fluorescent image stacks of bloodvessels (green) and labeled tumor cells (red) are shown. Graph shows % of injected embryos showing either of the two typical types of tumor cell migration patterns (15 embryos per condition analyzed).

	shβ1#1	shβ1#2
Cdh1	-4.1; 3.25e-10	-6.67; p=8.56e-11
Snail1	1.22; p=0.026	1.13; p=0.27
Snail2; Slug	1.10; p=0.35	1.02; p=0.73
Twist1	1.39; p=0.019	1.86; p=7.09e-8
Twist2	-1.13; p=0.022	-1.02; p=0.75
Zeb1	-1.03; p=0.57	1.21; p=0.0051
Zeb2	1.97; p=7.33e-5	2.45; p=2.56e-4
Tcf3; E2A; E12/E47	1.01; p=0.84	-1.05; p=0.55

Figure S6. Micro-array analysis of E-cadherin and indicated E-cadherin repressors in two independent 4T1shβ1 lines. Fold change compared to control group (4T1 wild type and 4T1 sh-control) and p-value is shown. Genes showing significant change (p<0.001) are indicated in blue.

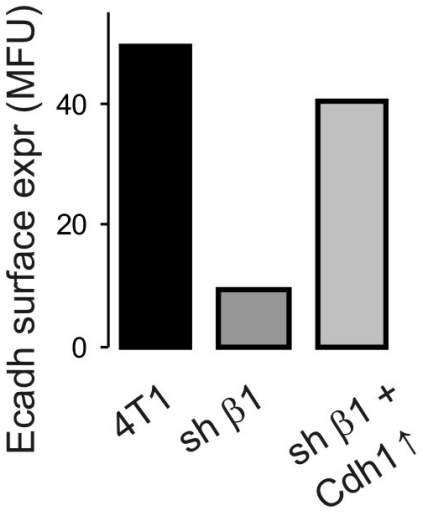

Figure S7. FACS analysis of E-cadherin surface expression in 4T1 cells expressing indicated shRNAs and cDNAs.

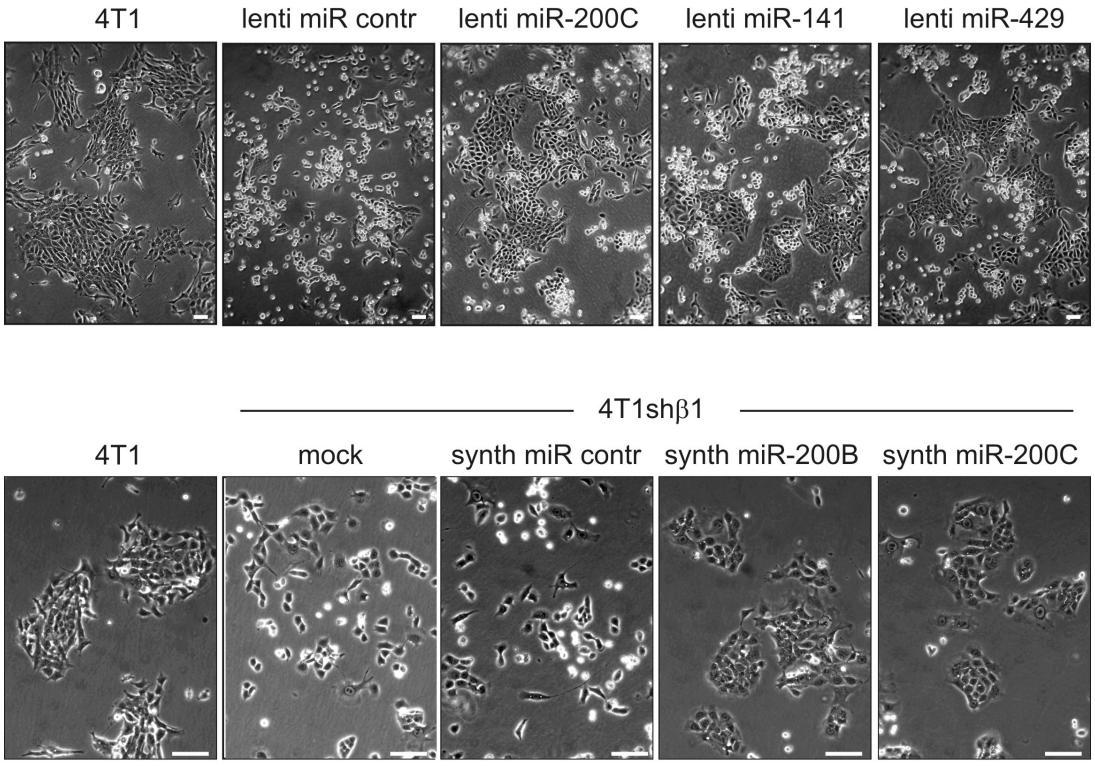

Figure S8. 4T1 cohesion in 2D culture suppressed by shβ1 and restored by lentiviral (top) or synthetic (bottom) expression of indicated miR-200 species. Scale bars, 50 μm.

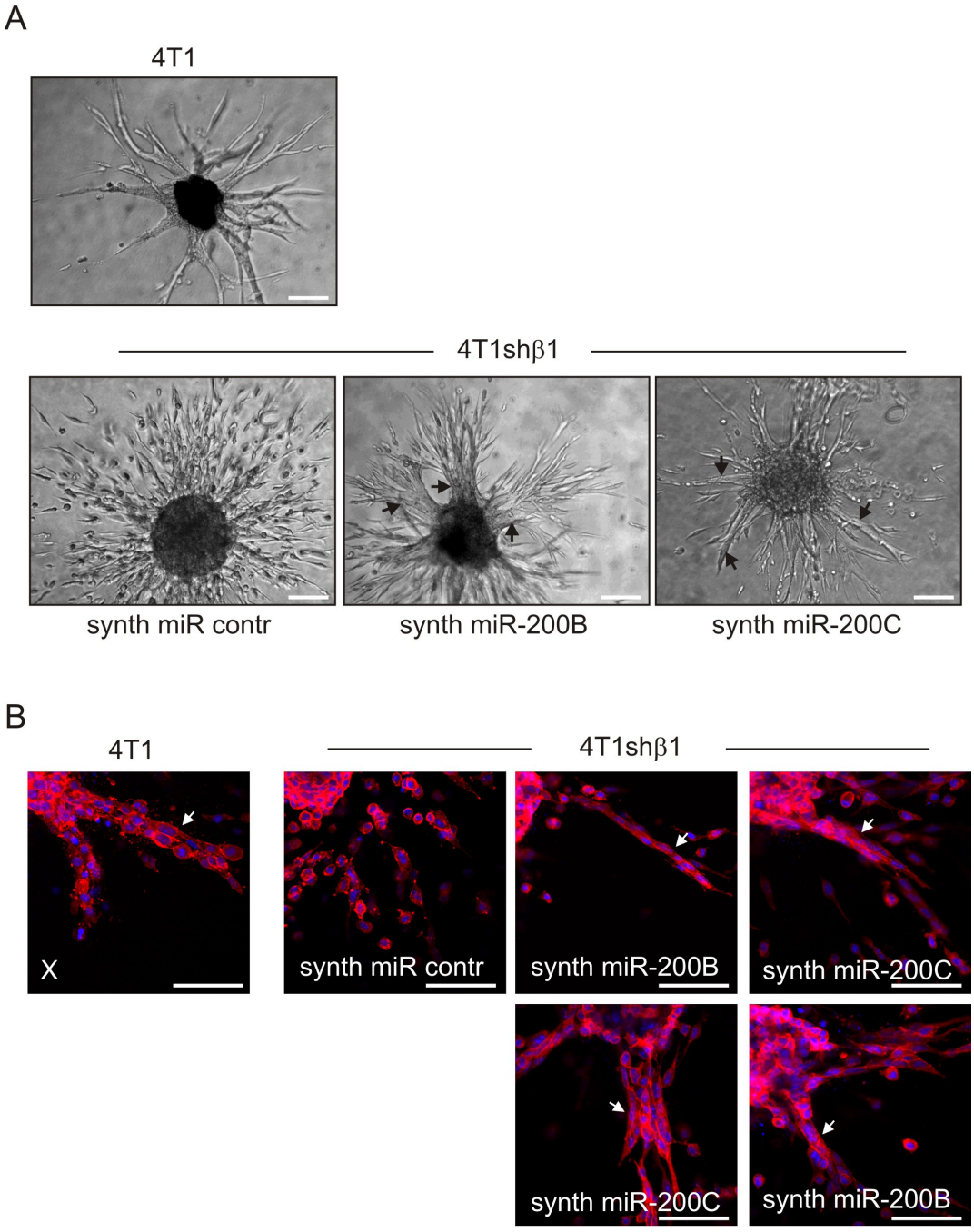

Figure S9. 4T1 cohesion in collagen gels suppressed by shβ1 and restored by synthetic expression of indicated miR-200 species. DIC (**A**) and actin & nuclear staining (Phalloidin & Hoechst; **B**) is shown. Arrows point to cohesive invasion strands. Scale bars, 50 μm.

Table S1: Differentially expressed genes shared between two independent 4T1shβ1 lines

Probe set	Gene symbol	fold-change shb1#1	fold-change shβ1#2
1428380_PM_at	0610007C21Rik	1.58	1.52
1429252_PM_at	0610010K14Rik	-1.81	-1.73
1447870_PM_x_at	1110002E22Rik	-2.06	-2.13
1435464_PM_at	1110003E01Rik	3.88	4.70
1442363_PM_at	1110012J17Rik	2.03	2.66
1434441_PM_at	1110018J18Rik	1.82	2.15
1431786_PM_s_at	1190003J15Rik	-2.64	-4.10
1429219_PM_at	1200009F10Rik	1.90	2.59
1428851_PM_at	1300014I06Rik	1.68	1.64
1442992_PM_at	130004C03	2.17	2.39
1417474_PM_at	1500035H01Rik	1.56	1.59
1439014_PM_at	1600021P15Rik	-1.51	-1.60
1429758_PM_at	1700017B05Rik	2.15	2.39
1423289_PM_a_at	1810029B16Rik	-1.52	-1.58
1454224_PM_at	2010300F17Rik	-3.26	-2.79
1424520_PM_at	2010305A19Rik	1.53	1.57
1453275_PM_at	2310002L13Rik	-16.31	-23.14
1428241_PM_at	2310035K24Rik	1.84	1.70
1429215_PM_at	2310058N22Rik	1.76	2.12
1428350_PM_at	2310061F22Rik	-2.14	-1.79
1428404_PM_at	2410025L10Rik	1.73	1.93
1434581_PM_at	2410066E13Rik	2.06	2.00
1436216_PM_s_at	2610204M08Rik	1.93	2.15
1426012_PM_a_at	2610301G19Rik	1.81	1.87
1429268_PM_at	2610318N02Rik	1.54	1.82
1424983_PM_a_at	2700078E11Rik	-1.73	-1.82
1418389_PM_at	2810453I06Rik	-1.98	-1.97
1432757_PM_at	2900011L18Rik	2.00	2.10
1444062_PM_at	2900056L01Rik	3.82	4.18
1436462_PM_at	3100002L24Rik	3.21	2.53
1452779_PM_at	3110006E14Rik	3.42	3.58
1458491_PM_at	4930422I07Rik	1.75	1.97
1441749_PM_at	4930447F24Rik	2.06	2.71
1435052_PM_at	4930455F23Rik	1.75	2.03
1429055_PM_at	4930506M07Rik	-1.72	-1.63
1454606_PM_at	4933426M11Rik	1.95	1.63
1432059_PM_x_at	5031425E22Rik	2.35	2.43
1430023_PM_at	5133400G04Rik	-1.54	-1.73
1435830_PM_a_at	5430435G22Rik	5.20	1.68
1454460_PM_at	5730433N10Rik	6.12	4.66
1441972_PM_at	6230424C14Rik	10.99	5.17
1439770_PM_at	6430598A04Rik	3.40	1.69
1454686_PM_at	6430706D22Rik	2.36	1.78
1433338_PM_at	6720460K10Rik	1.99	1.79
1429478_PM_at	6720463M24Rik	1.91	2.12
1428284_PM_at	8430427H17Rik	4.76	2.12
1430221_PM_at	9130008F23Rik	-3.27	-2.92
1415705_PM_at	9130011J15Rik	-1.61	-1.54
1436054_PM_at	9130227C08Rik	2.02	2.14
1436825_PM_a_at	A630095E13Rik	-3.59	-4.37
1424829_PM_at	A830007P12Rik	2.41	2.80
1435169_PM_at	A930001N09Rik	1.89	1.72
1453062_PM_at	A930026I22Rik	1.76	2.00
1440736_PM_at	AI131651	2.23	1.72
1456878_PM_at	AI646023	1.61	1.71
1455172_PM_at	AU020094	-2.04	-1.83
1452150_PM_at	AU040320	1.72	1.98
1455144_PM_s_at	AU040829	1.98	2.40
1458648_PM_at	AU042950	3.30	2.47
1423797_PM_at	Aacs	-1.72	-1.74
1451083_PM_s_at	Aars	-1.95	-1.72
1416402_PM_at	Abcb10	-1.66	-1.63
1428988_PM_at	Abcc3	4.06	3.46
1416014_PM_at	Abce1	-1.98	-1.66
1423570_PM_at	Abcg1	2.37	3.94
1439259_PM_x_at	Abhd4	1.73	1.52
1416946_PM_a_at	Acaa1a	2.44	2.93
1424184_PM_at	Acadvl	1.76	1.76
1439021_PM_at	Acap3	1.66	1.64
1424183_PM_at	Acat1	1.57	1.54
1425195_PM_a_at	Acat2	-1.58	-1.75
1429421_PM_at	Accs	1.66	1.63
1425326_PM_at	Acly	-2.55	-2.22
1436788_PM_at	Acp2	2.16	1.83
1456735_PM_x_at	Acpl2	2.83	3.12
1415873_PM_a_at	Actr1a	-1.57	-1.74
1419140_PM_at	Acvr2b	1.51	2.13
1417976_PM_at	Ada	-1.57	-1.90
1421172_PM_at	Adam12	-7.19	-11.30
1421858_PM_at	Adam17	1.56	1.70
1416871_PM_at	Adam8	-2.73	-2.23
1450716_PM_at	Adamts1	-9.42	-5.84
1437785_PM_at	Adamts9	6.21	7.75
1440668_PM_at	Adamtsl3	1.94	4.25
1423298_PM_at	Add3	-1.61	-1.85
1424393_PM_s_at	Adhfe1	2.77	1.70
1451992_PM_at	Adrbk1	-1.76	-1.79
1436870_PM_s_at	Afap1l2	8.48	3.43
1416645_PM_a_at	Afp	3.54	3.63
1434287_PM_at	Agpat5	-1.76	-1.69
1426670_PM_at	Agrn	-1.58	-1.54
1422631_PM_at	Ahr	2.84	2.26
1422184_PM_a_at	Ak1	1.68	1.82
1457032_PM_at	Ak5	2.62	3.60
1434764_PM_at	Akap11	1.65	1.63
1419706_PM_a_at	Akap12	-2.79	-2.31
1455870_PM_at	Akap2	1.60	1.63
1433905_PM_at	Akap7	-1.87	-1.93
1450455_PM_s_at	Akr1c12	10.84	4.73

1418672_PM_at	Akr1c13	14.47	6.23	1452370_PM_s_at	B230208H17Rik	-1.62	-1.88
1423364_PM_a_at	Aktip	-1.90	-1.99	1428568_PM_at	B230217C12Rik	2.66	2.10
1415836_PM_at	Aldh18a1	-2.63	-2.06	1436842_PM_at	B230380D07Rik	3.14	3.93
1418752_PM_at	Aldh3a1	10.72	5.07	1457043_PM_at	B3galtl	1.71	2.61
1415776_PM_at	Aldh3a2	2.18	1.88	1418014_PM_a_at	B4galt1	1.62	1.64
1448104_PM_at	Aldh6a1	2.00	2.04	1425934_PM_a_at	B4galt4	-1.80	-1.53
1460167_PM_at	Aldh7a1	2.18	2.43	1433617_PM_s_at	B4galt5	1.95	2.10
1419115_PM_at	Alg14	-1.83	-1.56	1460329_PM_at	B4galt6	-11.53	-5.34
1455887_PM_at	Alg8	1.70	1.63	1438635_PM_x_at	B930041F14Rik	2.30	1.84
1434601_PM_at	Amigo2	13.54	10.99	1427947_PM_at	B9d2	2.20	1.98
1430697_PM_at	Ammecr1	-2.24	-2.29	1434200_PM_at	BC010981	-1.59	-1.75
1434444_PM_s_at	Anapc1	1.79	1.55	1424360_PM_at	BC019943	-1.93	-1.70
1439066_PM_at	Angpt1	8.76	15.63	1455437_PM_at	BC033915	2.11	2.96
1448831_PM_at	Angpt2	1.99	1.54	1456929_PM_at	BC042782	2.42	4.11
1455090_PM_at	Angptl2	2.55	2.52	1435794_PM_at	BC050254	1.66	1.70
1453287_PM_at	Ankrd33b	2.76	5.11	1424117_PM_at	BC056474	-1.56	-1.53
1451182_PM_s_at	Ankrd54	1.68	1.60	1435209_PM_at	BC057079	-1.77	-1.53
1451446_PM_at	Antxr1	4.84	4.02	1424951_PM_at	Baiap2l1	-1.75	-1.79
1418468_PM_at	Anxa11	1.93	2.16	1453076_PM_at	Batf3	1.64	1.79
1460330_PM_at	Anxa3	-1.59	-1.50	1450622_PM_at	Bcar1	-1.89	-2.16
1416137_PM_at	Anxa7	1.52	1.74	1416647_PM_at	Bckdha	2.22	2.27
1460190_PM_at	Ap1m2	-3.42	-3.22	1419406_PM_a_at	Bcl11a	-2.40	-2.77
1447903_PM_x_at	Ap1s2	3.23	2.99	1420888_PM_at	Bcl2l1	1.60	1.67
1427077_PM_a_at	Ap2b1	-1.76	-2.01	1456006_PM_at	Bcl2l11	2.28	2.20
1422593_PM_at	Ap3s1	2.04	1.80	1452614_PM_at	Bcl2l15	-1.95	-2.60
1449070_PM_x_at	Apcdd1	7.71	13.26	1442187_PM_at	Bdkrb2	-2.83	-2.74
1456500_PM_at	Aph1b	1.78	2.27	1422169_PM_a_at	Bdnf	2.70	4.76
1416203_PM_at	Aqp1	23.48	9.06	1426489_PM_s_at	Bfar	1.55	1.63
1418818_PM_at	Aqp5	7.03	2.53	1418025_PM_at	Bhlhe40	-4.86	-7.41
1452291_PM_at	Arap2	-2.92	-8.37	1425532_PM_a_at	Bin1	1.82	1.82
1421134_PM_at	Areg	2.45	2.39	1417691_PM_at	Bin3	2.22	1.99
1418847_PM_at	Arg2	2.58	3.03	1426238_PM_at	Bmp1	1.58	1.52
1426952_PM_at	Arhgap18	6.87	5.56	1418910_PM_at	Bmp7	-3.06	-2.58
1435108_PM_at	Arhgap22	2.10	2.17	1416923_PM_a_at	Bnip3l	1.57	1.73
1435694_PM_at	Arhgap26	1.87	2.05	1435480_PM_at	Braf	-2.09	-2.06
1434809_PM_at	Arhgap28	3.07	3.10	1448521_PM_at	Brd7	-1.67	-1.51
1454745_PM_at	Arhgap29	-2.49	-1.86	1427270_PM_a_at	Bsdc1	1.73	1.86
1451867_PM_x_at	Arhgap6	5.99	4.61	1435249_PM_at	Btaf1	-2.03	-1.70
1448660_PM_at	Arhgdig	-2.25	-1.58	1424054_PM_at	Btbd2	2.05	1.63
1421164_PM_a_at	Arhgef1	-1.51	-1.83	1417987_PM_at	Btd	1.83	1.96
1424250_PM_a_at	Arhgef3	-1.95	-3.81	1424074_PM_at	Btf3l4	1.67	2.07
1431429_PM_a_at	Arl4a	1.86	1.75	1426268_PM_at	C130090K23Rik	-2.05	-2.64
1427167_PM_at	Armcx4	-2.59	-3.90	1422772_PM_at	C1galt1	-1.93	-1.86
1454617_PM_at	Arrdc3	7.73	7.49	1435580_PM_at	C230081A13Rik	2.74	3.75
1434961_PM_at	Asb1	2.34	1.82	1436709_PM_at	C230096C10Rik	1.79	1.83
1423422_PM_at	Asb4	-3.38	-3.65	1457046_PM_s_at	C77370	-1.89	-1.94
1451095_PM_at	Asns	-2.35	-1.87	1446288_PM_at	C78692	2.15	2.13
1448763_PM_at	Atad1	-1.78	-1.99	1441673_PM_at	C80120	1.75	2.20
1449363_PM_at	Atf3	-3.57	-3.31	1440513_PM_at	C80258	1.91	2.51
1451747_PM_a_at	Atg12	2.00	1.73	1453232_PM_at	Calr3	1.71	1.98
1434092_PM_at	Atg9b	-2.76	-3.27	1452050_PM_at	Camk1d	3.29	6.73
1456388_PM_at	Atp11a	-1.61	-1.59	1439168_PM_at	Camk2d	1.82	1.55
1452746_PM_at	Atp13a2	1.53	1.62	1423941_PM_at	Camk2g	2.39	1.92
1436921_PM_at	Atp7a	2.15	2.12	1439843_PM_at	Camk4	2.00	2.73
1418774_PM_a_at	Atp7a	2.15	2.00	1426901_PM_s_at	Camta2	1.92	2.03
1434026_PM_at	Atp8b2	2.17	1.98	1437537_PM_at	Casp9	1.75	1.86
1415932_PM_x_at	Atp9a	1.73	2.00	1449145_PM_a_at	Cav1	-2.48	-2.66
1453681_PM_at	Atpif1	1.69	1.94	1422666_PM_at	Cblc	-1.73	-2.16

Movie S1. 4T1 cell migration in collagen gel (start 48h post injection; duration ~3h).

Movie S2. 4T1shβ1 cell migration in collagen gel (start 48h post injection; duration ~3h).

Movie S3. 4T1 cell migration in collagen gel incubated with VP12 (start 48h post injection; duration ~3h).

FULL METHODS

Cell lines and animals. 4T1 mouse breast cancer cells and MCF10a human mammary epithelial cells were obtained from ATCC and cultured according to the provided protocol. Rag2−/−;γc−/− mice were housed in individually ventilated cages under sterile conditions. Housing and experiments were performed according to the Dutch guidelines for the care and use of laboratory animals. Sterilized food and water were provided ad libitum. Zebrafish were maintained according to standard protocols (http://ZFIN.org). Embryos were grown at 28.5-30˚C in egg water (60 μg/ml Instant Ocean Salts). During injection with tumor cells, embryos were kept under anesthesia in 0.02% buffered 3-aminobenzoic acid ethyl ester (Tricaine, Sigma).

Antibodies and peptides. For FACS, primary antibodies included HMβ1 anti-mouse β1 (BD Pharmingen), AIIB2 anti-human β1, Ha1/29 anti-mouse α2 (BD Pharmingen), or DECMA anti-mouse/human E-cadherin (Sigma-Aldrich). For Western blot, primary antibodies included HMβ1 anti-mouse β1, 36/E-cadh anti-mouse/human E-cadherin (BD Transduction Laboratories), and B-5-1-2 anti-α-tubulin (Sigma). For immunohistochemistry on frozen tumor sections and in fixed collagen gels, 36/E-cadh anti-mouse/human E-cadherin antibody (BD Transduction Laboratories) was used. For tumor cell migration interference studies, snake venom-derived disintegrins and C-lectin type proteins, including Obustatin (α1β1), VLO4 (α5β1; αvβ3), VLO5 (α4β1; α9β1) and VP12 (α2β1), were used at a concentration of 4.6 μM[5].

Stable cDNA and shRNA expression. 4T1 and MCF10a cells were transduced using lentiviral shRNA vectors (LentiExpress™; Sigma-Aldrich) according to the manufacturers' procedures and selected in medium containing 2 μg/ml puromycin. Control vectors included shRNA targeting TurboGFP (shc#1) and shRNA targeting eGFP (shc#2). shRNAs silencing mouse β1 integrin included those targeting *gcacgatgtgatgatttagaa* (shβ1#1; nucleotides 360-383 in the mouse *Itgb1* coding sequence) and *gccattactatgattatcctt* (shβ1#2; nucleotides 1111-1131 in the mouse *Itgb1* coding sequence). shRNAs silencing mouse α2 integrin included those targeting *gcgttaattcaatatgccaat* (shα2#1; nucleotides 733-753 in the mouse *Itga2* coding sequence) and *gcagaagaatatggtggtaaa* (shα2#2; nucleotides 2274-2294 in the mouse *Itga2* coding sequence). shRNAs silencing human β1 integrin included those targeting *gccctccagatgacatagaaa* (shβ1#1; nucleotides 360-380 in the human *ITGB1* coding sequence) and *gccttgcattactgctgatat* (shβ1#2; nucleotides 2367-2387 in the human *ITGB1* coding sequence). 4T1shβ1 cells were transduced with pCSCG/mECAD lentiviral cDNA expression vector for mouse E-cadherin (provided by Dr. Patrick Derksen, University Medical Center, Utrecht NL). Cells transduced with integrin shRNAs or E-cadherin cDNA were selected for

stable knockdown or stable expression phenotypes, respectively by two rounds of bulk FACS sorting (see below for technical details).

Lentiviral expression of miRNA shMimics.
4T1shβ1 cells were transduced using miRIDIAN shMIMIC Lentiviral miRNAs (non-targeting control, miR-200a, miR-200b, miR-200c, miR-141, and miR-205; ThermoFisher Scientific) according to the manufacturers' procedures followed by two rounds of bulk sorting for GFP expression. Subsequently, cells were used for E-cadherin FACS, qPCR analysis, or collagen invasion studies.

Transfection of synthetic miRNA Mimics, and miRNA Hairpin Inhibitors.
Cells were seeded at 5x105 cells per well in 12 wells plates and transfected at a final concentration of 50 nM of miRIDIAN miRNA Mimics (ThermoFisher Scientific; control non-targeting, miR-200a, miR-200b, miR-200c, miR-141, and miR-205), or miRIDIAN miRNA Hairpin Inhibitors (ThermoFisher Scientific; control non-targeting, miR-200a, miR-200b, miR-200c, miR-141, and miR-205) using DharmaFECT2 (ThermoFisher Scientific). Cells were replated 24 hours post transfection and used for E-cadherin FACS, qPCR analysis, or collagen invasion 48 hours later.

Luciferase reporter assay. 4T1 wild type and 4T1shβ1 cells were transiently transfected with 10 ng of an E-cadherin firefly luciferase reporter plasmid[21] (provided by Dr. Geert Berx, VIB, Gent BE) and 2 ng of a CMV-renilla luciferase reporter using lipofectamine plus (Invitrogen) and analyzed using a dual luciferase kit (Promega) 3 days later, according to the manufacturers' procedure.

3D invasion assays. Cell suspensions in PBS containing 2% polyvinylpyrrolidone (PVP; Sigma-Aldrich) were microinjected (~$1x10^4$ cells/droplet) using an air driven microinjector (20 psi, PV820 Pneumatic PicoPump; World precision Inc) into collagen gels prepared from 2.5 mg/ml acid-extracted rat tail collagen type 1. Tumor cell spheroids were monitored for 4 days. For immunostaining at 4 days post-injection, gels were incubated for 30 min with 5 µg/ml collagenase (from Clostridium histolyticum, Boehringer Mannheim) at room temperature, fixed with 4% paraformaldehyde, permeabilized in 0.2% Triton X-100, and blocked with 1% BSA. Gels were incubated with Rhodamin-conjugated Phalloidin or with E-cadherin antibody followed by Alexa 488-conjugated secondary antibody and Hoechst nuclear staining. Preparations were mounted in Aqua-Poly/Mount solution (Polysciences, Inc) and analyzed using a Nikon TE2000 confocal microscope. Z-stacks (50 x 1 µm) were obtained using a 20x dry objective and converted into a single Z projection using the "extended depth of field" plugin from ImageJ software.

For real time imaging, ~3 hours time-lapse movies of spheroids were obtained starting at 48 hours post-injection. Image acquisition was performed using a Nikon TE2000 confocal microscope with a temperature and CO_2 controlled incubator. Differential interference contrast (DIC) time-lapse videos were recorded using a charged coupled device (CCD) camera controlled by NIS Element Software. Images were converted into a single avi file in Image-Pro Plus (Version5.1; Media Cybernetics).

Mouse orthotopic transplantation experiments. $1×10^5$ tumor cells in 0.1 mL PBS were injected

into the fat pad of 8-12-week old female Rag2$^{-/-}$;γc$^{-/-}$ mice. Size of the primary tumors was measured using calipers. Horizontal (*h*) and vertical (*v*) diameters were determined and tumor volume (*V*) was calculated: $V = 4/3\pi\{1/2[\sqrt{}(h \times v)]^3\}$. After 3-4 weeks, animals were anesthetized with pentobarbital and primary tumor and lungs were excised. Primary tumor and left lung were divided into two pieces that were snap frozen in liquid nitrogen for E-cadherin immunostaining or fixed in 4% paraformaldehyde for H&E staining. For counting of lung metastases, right lungs were injected with ink solution, destained in water, and fixed in Feketes [4.3% (vol/vol) acetic acid, 0.35% (vol/vol) formaldehyde in 70% ethanol]. To analyze circulating tumor cells in some mice blood was drawn from the right atrium via heart puncture after anesthetizing but before excision of primary tumor and lungs. 0.2 ml of blood was plated into 60-mm tissue culture dishes filled with growth medium. After 5 days, tumor cell clones were stained using MTT (Sigma) and counted using ImageJ.

Zebrafish xenotransplantation experiments. For quantification of tumor cell spreading, tumor cells were labeled with CM-DiI (Invitrogen), mixed with 2% PVP, and injected into the yolk sac of enzymatically dechorionated, two-day old Fli-GFP transgenic zebrafish embryos using an air driven microinjector (20 psi, PV820 Pneumatic PicoPump; World precision Inc). Embryos were maintained in egg water at 34°C for 6 days and subsequently fixed with 4% paraformaldehyde. Imaging was done in 96 well plates containing a single embryo per well using a Nikon Eclipse Ti confocal laser-scanning microscope. Z stacks (15 x 30 μm) were obtained using a Plan Apo 4X Nikon dry objective with 0.2 NA and 20 WD. Images were converted into a single Z projection in Image-Pro Plus (Version 6.2; Media Cybernetics). Automated quantification of cumulative tumor cell spreading per embryo was carried out using an in-house built Image-Pro Plus plugin.
For analysis of tumor cell migration strategies, labeled tumor cells were injected in the developing blood system and clusters of cells trapped in the vasculature were imaged 3 days post injection. Z stacks (75 x 1 μm) were obtained using a Plan Apo 20X Nikon dry objective with 0.2 NA and 20 WD.

mRNA and miRNA analysis. Total RNA for qPCR and miRNA profiling was extracted using Trizol (Invitrogen). cDNA was randomly primed from 50 ng total RNA using iScript cDNA synthesis kit (BioRad) and real-time qPCR was subsequently performed in triplicate using SYBR green PCR (Applied Biosystems) on a 7900HT fast real-time PCR system (Applied Biosystems). The following qPCR primer sets were used: β-actin, forward *aacctggaaaagatgacccagat* reverse *cacagcctggatggctacgta*; E-cadherin, forward *atcctcgccctgctgatt* reverse *accaccgttctcctccgta*; Zeb1, forward *ccttcaagaaccgctttctgtaaa* reverse *cataatccacaggttcagttttgatt*; Zeb2, forward *cagcagcaagaaatgtattggtttaa*, reverse *tgtttctcattcggccatttact*. Data were collected and analysed using SDS2.3 software (Applied Biosystems). Relative mRNA levels after correction for β-actin control mRNA, were expressed using 2^(-ΔΔCt) method.

Detection of mature miRNAs was performed using Taqman microRNA qPCR assay kit according to the manufacturer's instructions (Applied Biosystems). The U6 small nuclear RNA was used as internal control.

For micro-arrays, total RNA was extracted using mirVana RNA isolation kit (Ambion Inc). RNA quality and integrity was assessed with Agilent 2100 Bioanalyzer system (Agilent technologies). The Affymetrix 3' IVT-Express Labeling Kit was used to synthesize Biotin-

labeled cRNA and this was hybridized to an Affimetrix MG430 PM Array plate. Data quality control was performed with Affymetrix Expression Console v1.1 and all raw data passed the affimetrix quality criteria. Median normalization of raw expression data and identification of differentially expressed genes using a random-variance t-test was performed using BRB ArrayTools[23] version 4.1.0 Beta 2 release (developed by Dr. Richard Simon and BRB-ArrayTools Development Team members; http://linus.nci.nih.gov/BRB-ArrayTools.html). Annotation was done according to the NetAffx annotation date release 2009-11-23. Corrections for multiple testing were performed as described by calculating the FDRs[24].

Western blot and flow cytometry. For Western blot, cells were lysed with modified RIPA buffer (150 mM NaCl, 1.0% triton-X 100, 0.5% Na deoxycholate, 0.1% 50mM Tris pH 8, and protease cocktail inhibitor (Sigma-Aldrich)). Samples were separated on SDS PAGE gels and transferred to PVDF membranes (Millipore), incubated with primary antibodies followed by horseradish peroxidase-labeled secondary antibodies (Jackson ImmunoResearch Laboratories inc), and developed with enhanced chemiluminescence substrate mixture (ECL plus, Amersham, GE Healthcare). Blots were scanned on a Typhoon 9400 (GE Healthcare).

For flowcytometry, cells were detached either using trypsin/EDTA (in the case of GFP or integrin surface expression) or by 0.02% EDTA only (in the case of E-cadherin surface expression). Surface expression levels were determined using primary antibodies, followed by fluorescence-conjugated secondary antibodies, and analysis on a FACSCanto or sorting on a FACSCalibur (Becton Dickinson).

Statistical analysis. Data are presented as mean ± SEM of at least 3 independent biological replicates unless otherwise stated. Student's t test (two-tailed) was used to compare groups.

References to full methods.

23. Wright G.W. and Simon R. (2003) A random variance model for detection of differential gene expression in small microarray experiments. *Bioinformatics* 19:2448-2455.
24. Benjamini, Y. and Hochberg, Y. (1995) Controlling the false discovery rate: a practical and powerful approach to multiple testing. *J Royal Stat Soc*, Series B (Methodological) 57:289–300.